Tracing Memory Effects in Correlated Diffusion Anisotropy in MFI-Type Zeolites by MD Simulation

Siegfried Fritzsche*,† and J. Kärger‡

University Leipzig, Institute for Theoretical Physics, Augustusplatz 9-11, D-04109 Leipzig, Germany, and University Leipzig, Institute for Experimental Physics I, Linnestrasse 53, D-04103 Leipzig, Germany

Received: July 16, 2002; In Final Form: November 22, 2002

The correlation between the principal tensor elements of diffusion in MFI-type zeolites such as silicalite-1 and ZSM-5 may be substantially affected by memory effects. Extensive MD simulations of the molecular diffusion of methane in zeolite silicalite-1 are analyzed on the basis of the concept of memory-dependent molecular propagation. The obtained results are in good agreement with analytical approaches to memory effects presented in the literature.

1. Introduction

The structure-related interdependence of the principal elements of the diffusion tensor is a remarkable feature of molecular propagation in zeolites.[1−4] In the case of MFI-type zeolites, for example, the diffusivities in the main crystallographic directions are found to obey a first-order approximation of the relation[1,4]

$$\frac{c^2}{D_z} = \frac{a^2}{D_x} + \frac{b^2}{D_y} \tag{1}$$

with a, b, and c denoting the unit cell extensions in the x, y, and z directions.

As can be seen from the schematic representation of the pore network of silicalite-1 in Figure 1, there are straight and zigzag channels in the y and x directions, but there is no equivalent direct diffusion pathway in the z direction. Instead, molecular propagation in the z direction is realized by subsequent moves in the x direction, which has a z component. To lead to a shift larger than $c/2$, they have to be interrupted by moves in the y direction to another zigzag channel because otherwise the z components of subsequent moves in the x direction cancel each other. The only assumption in the derivation of eq 1 was that subsequent moves between intersections are statistically independent from each other. This means that a molecule passing a channel intersection continues on its way independent of its past (i.e., independent of the channel intersection from where it has come). Although in numerous experimental[5,6] and simulation[7−13] studies eq 1 was found to serve as a reasonable estimate, in several cases the deviations were found to be physically significant.

The requirement of memoryless propagation cannot be maintained, therfore, as a general supposition of molecular propagation in MFI-type zeolites.

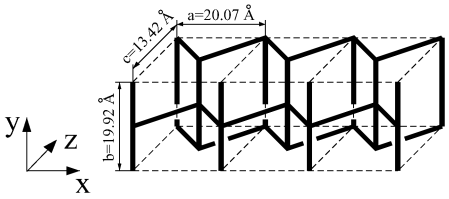

Figure 1. Topology of the channels in silicalite-1.

In ref 7, the deviations of the interelation between the principal tensor elements and eq 1 were quantified by introducing a memory parameter

$$\beta = \frac{c^2/D_z}{a^2/D_x + b^2/D_y} \tag{2}$$

Obviously, eqs 1 and 2 coincide with $\beta = 1$, so this case corresponds to molecular propagation without memory. The case of $\beta > 1$ refers to molecular propagation where subsequent displacements are more likely to occur in one and the same channel. As a consequence, molecular propagation in the z direction (which is only possible by interchanges between the two channel types) is reduced. As an extreme case of this situation, for the interpretation of the frequency response patterns observed for the diffusion of 2-butyne and *p*-xylene in silicalite-1,[14,15] it has been postulated, for example, that the diffusants remain in one and the same channel type over the total time of the experiment. Such a behavior would clearly correspond to $D_z = 0$ and hence to $\beta = \infty$. However, $\beta < 1$ would imply that interchanges of the diffusants between the segments of different channel types occur more frequently than random.

In ref 13, conditional probabilities have been introduced to treat this problem. In ref 16, memory effects on particle propagation in pore networks of the MFI structure type have been quantified by a similar set of probabilities that have been developed to explicit expressions for the components of the diffusion tensor and the memory parameter β. Reproducing eq 1 as a limiting case, the thus-established correlation rule of diffusion anisotropy represents the more general case of correlation between the principal elements of the diffusion tensor

* Corresponding author. E-mail: siegfried.fritzsche@physik.uni-leipzig.de.
† University Leipzig, Institute for Theoretical Physics.
‡ University Leipzig, Institute for Experimental Physics I.

10.1021/jp026541n CCC: $25.00
Published on Web 03/19/2003

in zeolites of the MFI-type structure. In the present paper, the validity of this generalized correlation rule of zeolite diffusion shall be confirmed by extensive MD simultions. The results of ref 13 are compared with those of the simpler treatment given in ref 16.

The paper is organized in the following way. After introducing a set of probabilities describing the memory effect in molecular propagation, section 2 recollects the main features of the analytical derivation of the correlation rule of diffusion anisotropy with memory effects given in ref 16. Section 3 describes the molecular dynamics (MD) simulations of the diffusion of methane as a model diffusant in the pore network of MFI and their analysis in terms of the introduced propagation probabilities. A comparison between the MD results and the predictions of the analytical treatment is given in section 4. As a measure of correlation effects, in section 5 the autocorrelation functions of subsequent displacements are considered.

2. Representing the Memory Parameter of Diffusion in MFI by a Set of Propagation Probabilities

Most of the MD simulations of molecular propagation in MFI-type channel networks did not yield complete agreement with the simple correlation rule, eq 1, so the underlying assumption of uncorrelated periods of propagation between subsequent channel intersections cannot be maintained. In refs 9−11, the particle memory was taken account of by considering pairs of subsequent displacements in a "two-step model". In this way, particle memory was extended over the period of two steps but not any longer. It was not unexpected, therefore, that the agreement between the MD simulations and the analytical estimates on the basis of the two-step model was still unsatisfactory.

Remarkable progress was made in ref 13, where conditional probabilities were introduced for correlation effects in the treatment of the diffusion of ethane in silicalite-1. It is the merit of this paper to have initiated the examination of the correlated diffusion of guest molecules in silicalite-1 channels by conditional probabilities.

Unfortunately, explicit expressions for the components of the diffusion tensor are given only for the limiting case without memory. In the more general case, these components can be calculated with the help of several other quantities that must be evaluated first. These quantities also allow for physical interpretations. The correlation parameter β is not investigated in ref 13.

An alternative method that also uses conditional probabilities was developed in ref 16. The expressions for the components of the diffusion tensor and β given in ref 16 allow for a power expansion that leads to a relatively simple expression for β, which allows for an interpretation of the deviation from random-walk behavior.

The significance of the conditional probabilities used in ref 16 and the present paper is schematically illustrated by Figure 2: The quantity $p_{x,x}$ represents the probability that a molecule, which has passed a segment of a zigzag channel from intersection to intersection, will continue its diffusive path in the same direction, and the next intersection where it shall arrive is that further on in the x direction. Correspondingly, the parameters $p_{x,-x}$ and $p_{x,y}$ represent the probabilities that the displacements to the next intersections are oriented backward or along a y channel segment, respectively.

The probabilities $p_{y,y}$, $p_{y,-y}$, and $p_{y,x}$ are defined in an analogous way. Since switches from one channel to the other one occur with the same probability, we clearly have $p_{x,y} \equiv p_{x,-y}$ and $p_{y,x} \equiv p_{y,-x}$, so there is no need to involve the two quantities on the right-hand side of these identities explicitly.

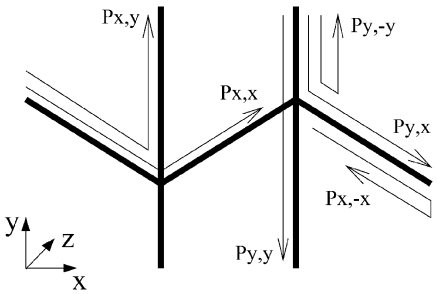

Figure 2. Illustration of the transition probabilities.

Normalization of the probabilities implies

$$p_{x,x} + p_{x,-x} + 2p_{x,y} = p_{y,y} + p_{y,-y} + 2p_{y,x} = 1 \qquad (3)$$

As the main feature in both the papers[1,3,4] and in the advanced access provided by refs 13 and 16, the diffusion paths are represented by a sequence of displacements along the elements of the straight and zigzag channels. In refs 1, 3, and 4, the quantities $p_{1(2)}$, in which an arbitrarily selected element belonged to a straight (zigzag) channel, turned out to be the sole parameters describing the total scenario of molecular propagation. With the parameter sets $p_{x,x}$, ..., $p_{y,y}$ introduced in ref 16, these displacements are now assumed to be correlated. The interelation between this parameter set and the probabilities p_i may be derived by appreciating the stationary condition

$$p_1 = p_1(p_{y,y} + p_{y,-y}) + 2p_2p_{x,y} \qquad (4)$$

$$p_2 = p_2(p_{x,x} + p_{x,-x}) + 2p_1p_{y,x} \qquad (5)$$

Equations 4 and 5 require that, on passing from an arbitrarily selected element of displacement in the trajectory to the subsequent one, again, with the probability $p_{1(2)}$, it must be an element of a straight (zigzag) channel. Their rearrangement yields

$$p_1 = \frac{2p_{x,y}}{2 - (p_{x,x} + p_{x,-x} + p_{y,y} + p_{y,-y})} \qquad (6)$$

$$p_2 = \frac{2p_{y,x}}{2 - (p_{x,x} + p_{x,-x} + p_{y,y} + p_{y,-y})} \qquad (7)$$

whose form may be further modified by the use of eq 3.

For particles without memory, we have

$$p_{y,y} = p_{y,-y} = p_{x,y} = \frac{p_1}{2} \qquad (8)$$

$$p_{x,x} = p_{x,-x} = p_{y,x} = \frac{p_2}{2} \qquad (9)$$

so the general treatment in ref 16 clearly involves the special case considered in refs 1−4.

The derivation of the correlation rule between the principal elements of the diffusion tensor is based on the 1D Einstein relation

$$D_x = \frac{\langle x^2(t)\rangle}{2t} \qquad (10)$$

with $\langle x^2(t)\rangle$ denoting the molecular mean-square displacement during t and with the corresponding equations for y and z. In ref 13, the trajectory is split into sequences of moves that take place in one and the same channel type. These sequences are treated separately. Instead, a different way is employed in ref 16 and in the present paper. The molecular displacements may be represented by the squares over the sums of the individual displacements $l_{x(y,z)i}$ from intersection to intersection

$$\langle x^2(t)\rangle = \langle(\sum_{i=1}^{n_x} l_{xi})^2\rangle \tag{11}$$

$$\langle y^2(t)\rangle = \langle(\sum_{i=1}^{n_y} l_{yi})^2\rangle \tag{12}$$

$$\langle z^2(t)\rangle = \langle(\sum_{i=1}^{n_z} l_{zi})^2\rangle \tag{13}$$

with $|l_{xi}|$, $|l_{yi}|$ and $|l_{zi}|$ being equal to $^a/_2$, $^b/_2$, and $^c/_2$, respectively, and n_x and n_y denoting the total number of "steps" along the zigzag channels (i.e., in the x direction) and along the straight channels (i.e., in the y direction), respectively. The probability of finding a particular one in a sequence of displacements is proportional to their number. Therefore, one has

$$\frac{n_y}{n_x} = \frac{p_1}{p_2} \tag{14}$$

Since, as a consequence of the channel shape, only steps in the z direction occur simultaneously with steps in x direction, we have $n_z = n_x$.

By making use of the formalism developed for the determination of correlation factors for the diffusion in solids,[17,18] in ref 16, the expressions on the right-hand sides of eqs 11−13 were evaluated and referred to the absolute values $^a/_2$, $^b/_2$, and $^c/_2$ of the displacement from intersection to intersection and the above-introduced set of probabilities.

The mean-square displacements are calculated by using the relation[17,18]

$$\langle(\sum_{i=1}^{n} l_i)^2\rangle = nl^2 + 2\sum_{i=1}^{n-1}\langle l_i l_{i+1}\rangle + 2\sum_{i=1}^{n-2}\langle l_i l_{i+2}\rangle + \ldots \tag{15}$$

with n standing for n_x, n_y, or n_z, l standing for a, b, or c and l_i standing for l_{xi}, $l_{yi,}$ or l_{zi}. The mean values of the products of subsequent displacements $\langle l_i l_{i+1}\rangle$ have to be treated separately for displacements within one channel type (i.e., in x and y directions) and for the z direction.

As soon as a molecule changes from one channel type to the other, previous displacements along this channel are not correlated anymore with future ones along the same channel. Subsequent displacements in x and y directions are thus easily found to obey the relations

$$\langle l_{xi} l_{x(i+j)}\rangle = (p_{x,x} - p_{x,-x})^j a^2 \tag{16}$$

$$\langle l_{yi} l_{y(i+j)}\rangle = (p_{y,y} - p_{y,-y})^j b^2 \tag{17}$$

Although the probabilities $p_{x,x}$ and $p_{x,-x}$ ($p_{y,y}$ and $p_{y,-y}$) for subsequent displacements along the crystallographic x (y) coordinates that are parallel- or antiparallel-directed are given by the very model applied, the equivalent probabilities p_+ and p_- for displacements in the z direction have to be provided by additional consideration. It may be deduced from Figure 1 that subsequent displacements in the z direction are oriented antiparallel (parallel) if they are separated by an even (odd) number of displacements along the straight channels. Summing over all probabilities belonging to either of the two cases yields

$$p_- = p_{x,x} + p_{x,-x} + 4p_{x,y}p_{y,x}(p_{y,y} + p_{y,-y})\sum_{i=0}^{\infty}[(p_{y,y} + p_{y,-y})^2]^i \tag{18}$$

$$p_+ = 4p_{x,y}p_{y,x}\sum_{i=0}^{\infty}[(p_{y,y} + p_{y,-y})^2]^i \tag{19}$$

Equations 18 and 19 may be transformed into

$$p_- = \frac{2(1 - p_{y,x} - p_{x,y})}{1 + p_{y,y} + p_{y,-y}} \tag{20}$$

$$p_+ = \frac{2p_{x,y}}{1 + p_{y,y} + p_{y,-y}} \tag{21}$$

As a final result, the principal tensor elements were found for sufficiently large n_x and n_y to be given by the simple expressions

$$D_x = \frac{a^2}{2t/n_x}\frac{1 + (p_{x,x} - p_{x,-x})}{1 - (p_{x,x} - p_{x,-x})} \tag{22}$$

$$D_y = \frac{b^2}{2t/n_y}\frac{1 + (p_{y,y} - p_{y,-y})}{1 - (p_{y,y} - p_{y,-y})} \tag{23}$$

$$D_z = \frac{c^2}{2t/n_x}\frac{p_{x,y}}{1 - p_{y,x} - p_{x,y}} \tag{24}$$

Inserting these relations into the expression of the correlation factor (eq 2) yields

$$\beta = \frac{p_1 C}{p_1 A + p_2 B} \tag{25}$$

with the notations

$$A = \frac{1 - (p_{x,x} - p_{x,-x})}{1 + (p_{x,x} - p_{x,-x})}$$

$$B = \frac{1 - (p_{y,y} - p_{y,-y})}{1 + (p_{y,y} - p_{y,-y})}$$

$$C = \frac{1 - p_{y,x} - p_{x,y}}{p_{x,y}}$$

To transform eq 25 into a form that explicitely reflects the interrelation between particle memory and the deviations from the no-memory case $\beta = 1$, a set of combined probabilities[16]

$$\Delta\pi_x = p_{x,x} - p_{x,-x} \tag{26}$$

$$\Delta\pi_y = p_{y,y} - p_{y,-y} \tag{27}$$

$$\Delta\pi_{x,y} = p_{x,x} + p_{x,-x} - 2p_{y,x} \tag{28}$$

has been introduced. $\Delta\pi_x$ and $\Delta\pi_y$ represent the probabilities that a molecule, which has arrived at a certain channel intersection, prefers to proceed to the subsequent intersection rather than to the preceding one, so their significance resembles that of the quantity χ in ref 13. Additionally, the quantity $\Delta\pi_{x,y}$

TABLE 1: Lennard-Jones Parameters σ (Å) and ϵ (kJ/mol) for the Derived[19] Spherical Averaged Model Potential

sorts	σ (Å)	ϵ (kJ/mol)
CH_4-Si	3.75	1.13
CH_4-CH_4	3.44	1.84
CH_4-O	3.37	0.63

compares the probabilities that on passing a channel intersection a molecule remains in the same channel type or moves to the other one.

Owing to eq 3, $\Delta\pi_{y,x}$ if introduced by analogy to eq 28 would coincide with $\Delta\pi_{x,y}$. If we use eqs 8 and 9, the right-hand sides of eqs 26−28 vanish in the no-memory case. Therefore, on considering only situations close to the no-memory case, it is sufficient to represent eq 25 as a function of $\Delta\pi_x$, $\Delta\pi_y$, and $\Delta\pi_{x,y}$ up to first order, yielding[16]

$$\beta \approx 1 + 2(p_y\Delta\pi_x + p_x\Delta\pi_y + \Delta\pi_{x,y}) \qquad (29)$$

3. MD Simulation

MD simulations have been carried out to check the theoretical model underlying the derivations and to test the validity of the equations derived above.

MD simulations[20,21] are a very useful tool in examining mechanisms of molecular motion because they give detailed insight and allow us to check relations and interdependencies by varying system parameters. A summary of recent developments in applying MD simulation to diffusion studies of guest molecules in zeolites may be found in review articles.[22−26]

The simulations for the present study have been carried out for a rigid lattice of pure silicalite-1 with methane as the guest molecule at a loading of 1 molecule per channel intersection (corresponding to 4 molecules per unit cell) and a temperature of 300 K. The effect of lattice vibrations on the diffusion of methane in silicalite-1 has been investigated in several papers,[27,28] and that of both lattice and molecule vibrations for the same system has been examined in ref 19. According to these studies, lattice vibrations should not be important for the present level of investigation of the correlation effect. Methane has been treated as a spherically shaped Lennard-Jones particle. This simplification has been used in many simulation studies of the diffusion of guest molecules in zeolites.[8,29−32] Various additional examples may be found in the review articles,[22−26] and we assume this model to be completely sufficient in examining the relation between basic jump probabilities and equations for the diffusion coefficients in different directions and their interdependencies.

The MD box contains two unit cells. Whereas in the *x* and *y* directions the edge lengths of the MD box agree with that of the unit cell, the edge length in the *z* direction is twice that of the unit cell in order to achieve a nearly cubic box. The edge lengths are 20.07, 19.92, and 26.84 Å, respectively. Periodical boundary conditions are applied to avoid finite size effects. The zeolite lattice consists of 576 lattice atoms that are arranged according to the geometry of the zeolites of type MFI.[33] The interaction parameters for the methane/lattice interaction are given in Table 1. They have been taken from the spherical model potential for methane derived in ref 19.

The trajectories have been calculated by the use of the velocity version of the Verlet algorithm.[20,21] In the present study, we have considered runs with an unperturbed evaluation part (after thermalization) of 5×10^6 simulation steps. The temperature was adjusted in the thermalization part of the run using a procedure described in refs 19 and 34 which enables us to carry out runs in the unperturbed microcanonical ensemble with deviations of only about 1% from a predefined value of the temperature. Because the time step was 5 fs, the length of the examined trajectory corresponded to a total time of 25 ns.

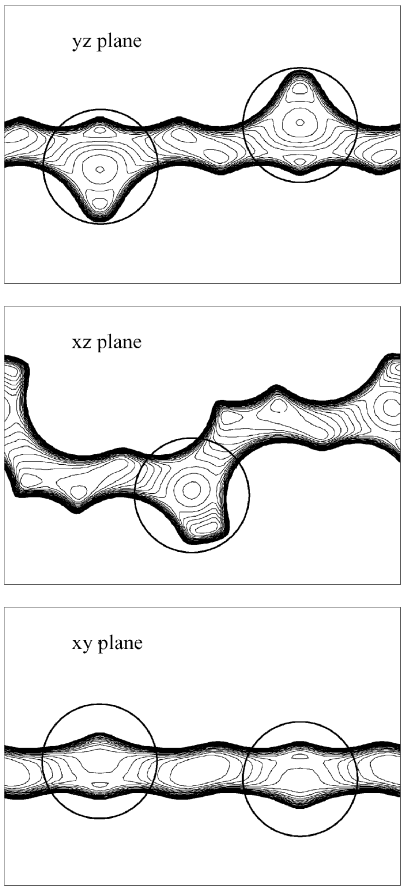

Figure 3. Definition of the intersection regions. The circles mark those regions that are treated as intersection regions. The highest energy connected with the outmost isopotential lines is −5 kJ/mol, whereas the lowest energy in small minima corresponds to about −25 kJ/mol.

The so-called channel intersections are parts of the zeolite void space that are shared by several channels. To decide whether a particle is in an intersection region, the limits of these regions must be declared. One possible choice is illustrated in Figure 3. It shows the isopotential lines for the center of a single methane molecule from the minimum of about −25 kJ/mol up to −5 kJ/mol in three planes: a cut through the straight channel in the *yz* plane at $x = 0$, a cut through the zigzag channel in the *xz* plane at $y = 0$, and a cut through the straight channel in the *xy* plane at $z = 0$. The circles correspond to cuts through spherical regions of radius 3 Å that can be interpreted as intersection regions. The position of the center of each such sphere is chosen in such a way that for a sphere radius of 3 Å all points in which a test molecule has a potential energy of less than −5 kJ/mol, and where the site of the molecule cannot be attributed to a single channel, are included in the sphere. This is illustrated by Figure 3. In Table 2, the Cartesian coordinates (in Å) of the sphere centers are given.

To investigate the influence of the size of the spheres considered to represent the intersection regions, the simulations have been analyzed by employing four different sphere radii.

4. Analysis of the MD Results in Terms of Particle Memory and the Correlation Rule

Table 3 provides a summary of the obtained simulation results. It particularly includes numerical values for all of the

TABLE 2: Coordinates (Å) of the Centers of the Spherical Regions That Are Considered to Represent the Channel Intersections

no.	*x*	*y*	*z*
1	9.635	4.980	−1.000
2	10.435	14.940	1.000
3	9.635	4.980	12.420
4	10.435	14.940	14.420
5	−0.400	4.980	7.710
6	0.400	14.940	5.710
7	−0.400	4.980	21.130
8	0.400	14.940	19.130

TABLE 3: Results of MD Simulations for Different Radii *r* of Intersection Regions[a]

r (Å)	2.0	2.5	3.0	5.0
$p_{x,x}$	0.19345	0.16695	0.13477	0.04369
$p_{x,-x}$	0.32031	0.43876	0.56070	0.87158
$p_{x,y}$	0.24078	0.19379	0.14724	0.04161
$p_{x,-y}$	0.24546	0.20050	0.15730	0.04313
$p_{y,y}$	0.37762	0.33034	0.26652	0.08525
$p_{y,-y}$	0.34844	0.43512	0.54964	0.86070
$p_{y,x}$	0.13891	0.11877	0.09365	0.02751
p_y	0.63348	0.61635	0.60295	0.59967
p_x	0.36547	0.37775	0.38350	0.39653
n_x	3634	4768	6661	30353
n_y	6443	8007	11023	47611
$\Delta\pi_x$	−0.12686	−0.27181	−0.42593	−0.82789
$\Delta\pi_y$	0.02918	−0.10478	−0.28312	−0.77545
$\Delta\pi_{x,y}$	0.23594	0.36816	0.50817	0.86023
D_x (no mem)	0.921	1.21	1.68	7.64
D_x (mem)	0.714	0.691	0.677	0.720
D_x (MD)	0.718	0.718	0.718	0.718
D_y (no mem)	1.61	1.99	2.74	11.81
D_y (mem)	1.70	1.62	1.53	1.49
D_y (MD)	1.68	1.68	1.68	1.68
D_z (no mem)	0.263	0.338	0.469	2.09
D_z (mem)	0.160	0.152	0.146	0.153
D_z (MD)	0.17	0.17	0.17	0.17
β (mem, eq 25)	1.40	1.42	1.42	1.41
β (mem, approx. 29)	1.33	1.32	1.29	1.11
β (MD, eq 2)	1.33	1.33	1.33	1.33
D_x [13]	0.706	0.685	0.672	0.718
D_y [13]	1.69	1.61	1.53	1.49
D_z [13]	0.160	0.154	0.150	0.155
β [13]	1.40	1.40	1.39	1.40

[a] The D values are 10^{-8} m^2/s. The notations no-mem, mem, and MD refer to data analysis without memory effects and with memory effects and to the MD data, respectively. The last four rows refer to estimates using our simulation data and the relations given in ref 13.

probabilities introduced in this study. To illustrate the data scattering, the values of both $p_{x,y}$ and $p_{x,-y}$ are presented. Ideally, they should coincide. Over the considered simulation runs, they are found to differ by only a few percent. The D values obtained from MD have been calculated from four moments of the displacement as described in ref 35 for the isotropic case and in ref 19 for the anisotropic case. In addition to these diffusivities from the MD simulations, Table 3 also contains diffusivity data, which would result from use of the Einstein relation together with eqs 11−13 if during their evaluation memory effects are neglected (case of no memory) or if memory effects are considered, as required by eqs 22−24. As a most impressive feature, the probability parameters are found to depend significantly on the size of the considered spheres in the intersection volumes. As expected, the probabilities for reversed propagation (i.e., passages from an intersection to the preceding one, as expressed by $p_{x,-x}$) strongly increase with increasing volume at the expense of continued propagation, as expressed by $p_{x,x}$ and $p_{y,y}$. This tendency is a consequence of the fact that with increasing sphere volumes the mean exchange rate from one intersection to the adjacent one and backward to the preceding one is clearly increasing. This is reflected by the dramatic increase in n_x and n_y in Table 3 with increasing radius.

As expected, deriving diffusivities from eqs 11−13 without taking into account the negative correlations between subsequent displacements (no-memory case) leads to quantities that are too large. Again, the error is larger with larger sphere radii. As stated above, they give rise to increasing numbers n_x or n_y of "apparent" steps and thus to sums in eqs 11−13 that are too large if the individual terms are considered to be uncorrelated. It is interesting that the quantities derived under the consideration of memory effects are far less affected by the size of the evaluation spheres. However, there is still a tendency that, as expected, the best agreement between the analytical estimates of D_x, D_y, and D_z (derived with the memory probabilities taken from the MD simulations) and the MD results themselves occurs for the smallest sphere volumes considered.

Correspondingly, the difference between the values of the memory parameter β given by eq 2 (with the diffusivities resulting from the MD simulations inserted) and by eq 25 drops to 5%. The remaining difference indicates that the introduced parameter set of probabilities does not yet represent a complete reflection of the propagation dynamics. Possible shortcomings might concern higher-order correlations or the interdependence of different states, which the diffusants may pass on their pathway along the various segments and intersections of the channel system. In this context, the complete agreement between the approximate expression, eq. 29, and the strict MD diffusivity-based relation, eq 25, has to be considered mere coincidence.

It is far more complicated to calculate diffusion coefficients from the relations presented in ref 13 than to using our eqs 22−24. To check the compatibility of the two treatments, we have subsequently used eqs 2, 35, 36, 44, 48, and 54 of ref 13 after having inserted our simulation results. The total simulation time is used for the division with t in eq 2. Thus, we were able to estimate the diffusivities and, via our eq 2, the memory parameter β. These results are also shown in Table 3. Irrespective of the different treatments, they show remarkably good agreement with the values obtained from eqs 22−24. (See Table 3.) That means that both treatments are employing memory effects at the same level of approximation.

On the basis of eq 29, the origin of the deviations of the memory parameter β from its no-memory value of 1 may be easily identified by means of the parameters $\Delta\pi_x$, $\Delta\pi_y$, and $\Delta\pi_{x,y}$, which are also displayed in Table 3. It turns out that the major mechanism leading to an enhancement of the memory parameter β is the enhanced probability to remain in one and the same channel on passing a channel intersection rather than to switch to the other channel type. This is documented by the substantial, positive values of $\Delta\pi_{x,y}$. In comparison with this mechanism, the fact that subsequent displacements along one and the same channel are more likely to be opposed to each other (leading to negative values of both $\Delta\pi_x$ for all sphere radii and $\Delta\pi_y$ for sphere radii larger than 2.0 Å and hence to a decrease in β according to eq 29) is of negligible influence.

5. Correlation Time

The question of whether it is sufficient to take into account only the correlation between two subsequent moves from intersection to intersection is closely related to the question of whether correlations over more than one such move exist. For one of the possible correlations, namely, the persistence of the

direction of subsequent moves in a given channel type, this has been proven by the following test.

To see the time schedule of the decay of such correlations, a quantity $H_x(i, \nu)$ has been introduced. $H_x(i,\nu)$ is equal to $+1$ if the νth change of intersection in the x direction of the ith particle happens in the positive x direction and -1 if it happens in the negative x direction. Only these two values are possible. Using this quantity $H_x(i, \nu)$, an autocorrelation function (ACF) $C_i(j)$ can be calculated from

$$C_i(j) = \sum_{\nu=1}^{M-j} H_x(i, \nu)\, H_x(i, \nu + j) \tag{30}$$

where M denotes the total number of particle shifts along the different channel elements in the considered direction. The functions $H_y(i, \nu)$ and $H_z(i, \nu)$ can be analogously defined.

In ref 36, similar correlation functions have been introduced and integrated to calculate diffusion coefficients. They have been used, however, to visualize the origin of shortcomings of the mean-field theory at higher concentrations rather than to discuss memory effects quantified and discussed in this paper. Contrary to ref 36, in the present paper the autocorrelation functions $C_i(j)$ are used only to illustrate the duration of the memory of particle jumps. Figure 4 shows the normalized ACFs of particle $i = 3$ for the run with sphere radius $=$ 3 Å. Figure 4 shows the necessity of considering memory effects in MFI-type channel networks in a most illustrative way. It can be seen that the memory decays rather slowly, attaining particularly large passage numbers j with respect to movements in the z direction. Besides possible memory effects, this can also be due to the fact that two subsequent moves in a zigzag channel always lead to alternating changes in the z coordinate that cancel each other. This is true if the second one has the same direction and also if it has the opposite direction. This is an example of a purely geometrical correlation.

The memory for movements in the z direction deserves particular recognition in view of the fact that propagation in the z direction appears to reflect features of anomalous diffusion over much larger time intervals than in the x and y directions.[37] However, the results given in ref 37 should be checked carefully because in a recent paper[38] the durations of the runs have been assessed to be too small to obtain reliable diffusion data. We ran a check for a β value less than 1.0 given in ref 37. Using the same interaction parameters as in that paper, in a test run for a concentration of 8 methane molecules per unit cell in silicalite-1 at 300 K, we found $\beta = 1.52$ (i.e., a value larger than 1.0 as in all cases reported in the present paper whereas in ref 37 a value of 0.6 has been obtained).

6. Conclusions

Though it has generally been accepted over the past decade that in several zeolite pore structures molecular propagation in different directions cannot occur independently from each other, so far any quantitative formulation of the interelation between the respective principal values of the diffusion tensor has been based on the rather crude assumption that subsequent displacements between characteristic ranges of the pore system (e.g., the channel intersections in the case of zeolite MFI) may occur independently of each other. In a new way of treatment of such phenomena initiated in ref 13, in ref 16 a parameter set of conditional probabilities has been introduced and used to establish an interrelation between the principal tensor elements with particular recognition of particle memory. In the present paper, MD simulations that illustrate the significance of this access and confirm its validity are reported. It is still an open question of whether the remaining difference of 5% between the values of the memory parameter β from the analytical expression and the simulation result reflects inherent minor shortcomings in the procedure. The expansion of the considerations to different loadings, temperatures, guest molecules, and host systems and the elucidation of the interdependence of the system parameters with the features of diffusion anisotropy leave ample space for challenging future research.

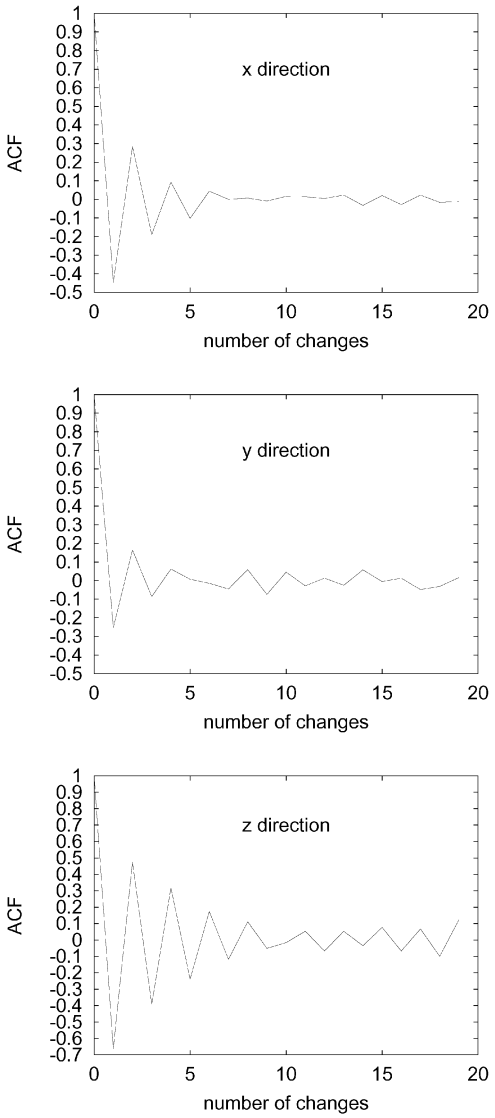

Figure 4. Normalized autocorrelation function (ACF) of H_x. Only integer values of j are possible. The lines connecting these points are guides for the eye.

Acknowledgment. We thank A. Schüring and S. Jost for fruitful discussions. Financial support by the Deutsche Forschungsgemeinschaft (SFB 294) and Fonds der Chemischen Industrie is gratefully acknowledged.

References and Notes

(1) Kärger, J. *J. Phys. Chem.* **1991**, *95*, 5558.

(2) Bär, N.-K.; Kärger, J.; Pfeifer, H.; Schäfer, H.; Schmitz, W. *Microporous Mesoporous Mater*. **1998**, *22*, 289.

(3) Fenzke, D.; Kärger, J. *Z. Phys. D: At., Mol. Clusters* **1993**, *25*, 345.

(4) Kärger, J.; Pfeifer, H. *Zeolites* **1992**, *12* 872.

(5) Caro, J.; Noack, M.; Richter-Mendau, J.; Marlow, F.; Petersohn, D.; Griepentrog, N.; Kornatowski, J. *J. Phys. Chem*. **1993**, *97*, 13685.
(6) Caro, J.; Noack, M.; Kölsch, K.; Schäfer, R. *Microporous Mesoporous Mater*. **2000**, *38*, 3.
(7) Maginn, E. J.; Bell, A. T.; Theodorou, D. N. *J. Phys. Chem*. **1996**, *100*, 7155.
(8) Jost, S.; Bär, N.-K.; Fritzsche, S.; Haberlandt, R.; Kärger, J. *J. Phys. Chem. B* **1998**, *102*, 6375.
(9) Kärger, J.; Demontis, P.; Suffritti, G. B.; Tilocca, A. *J. Chem. Phys*. **1999**, *110*, 1163.
(10) Demontis, P.; Kärger, J.; Suffritti, G. B.; Tilocca, A. *Phys. Chem. Chem. Phys*. **2000**, *2*, 1455.
(11) Demontis, P.; Suffritti, G. B.; Tilocca, A. *J. Chem. Phys*. **2000**, *113*, 7588.
(12) Vlugt, T. J. H.; Dellago, C.; Smit, B. *J. Chem. Phys*. **2000**, *113*, 8791.
(13) Jousse, F.; Auerbach, S. M.; Vercauteren, D. P. *J. Chem. Phys*. **2000**, *112*, 1531.
(14) Song, L.; Rees, L. V. C. *J. Chem. Soc., Faraday Trans*. **1993**, *89*, 1063.
(15) Song, L.; Rees, L. V. C. *J. Chem. Soc., Faraday Trans.* **1995**, *91*, 2027.
(16) Fritzsche, S.; Kärger, *J. Europhys. Lett.*, submitted for publication.
(17) Manning, J. R. *Phys. Rev.* **1959**, *116*, 819.
(18) Allnatt, A. R.; Lidiard, A. B. *Atomic Transport in Solids*; Cambridge University Press: Cambridge, U.K., 1993.
(19) Fritzsche, S.; Wolfsberg, M.; Haberlandt, R. *Chem. Phys.*, in press.
(20) Allen, M. P.; Tildesley, D. *Computer Simulation of Liquids*; Clarendon Press: Oxford, U.K., 1989.
(21) Haberlandt, R.; Fritzsche, S.; Peinel, G.; Heinzinger, K. *Molekulardynamik—Grundlagen und Anwendungen, mit einem Kapitel über Monte Carlo-Simulationen von H.-L. Vörtler*; Vieweg-Verlag: Wiesbaden, Germany, 1995.
(22) Haberlandt, R.; Fritzsche, S.; Vörtler, H. L. Simulation of Microporous Systems: Confined Fluids in Equilibrium and Diffusion in Zeolites. In *Handbook of Surfaces and Interfaces of Materials*; Nalwa, H. S., Ed.; Academic Press: San Diego, CA, 2001; Vol. 5, pp 358−444.
(23) Keil, F.; Krishna, R.; Coppens, M.-O. *Chem. Eng. J*. **2000**, *16*, 71.
(24) Bates, S.; van Santen, R. *Adv. Catal*. **1998**, *42*, 1.
(25) Demontis, P.; Suffritti, G. B. *Chem. Rev.* **1997**, *97*, 2845.
(26) Theodorou, D. N.; Snurr, R.; Bell, A. T. Molecular Dynamics and Diffusion in Microporous Materials. In *Comprehensive Supramolecular Chemistry* Alberti, G., Bein, T., Eds.; Pergamon Press: Oxford, U.K., 1996; Vol. 7, pp 507−548.
(27) Demontis, P.; Fois, E. S.; Suffritti, G. B.; Quartieri, S. *J. Phys. Chem*. **1990**, *94*, 4329.
(28) Demontis, P.; Fois, E.; Suffritti, G.; Quartieri, S. *J. Phys. Chem.* **1992**, *96*, 1482.
(29) Fritzsche, S.; Wolfsberg, M.; Haberlandt, R. *Chem. Phys.* **2000**, *253*, 283.
(30) Gaub, M.; Fritzsche, S.; Haberlandt, R.; Theodorou, D. N. *J. Phys. Chem. B* **1999**, *103*, 4721.
(31) Fritzsche, S.; et al. *Chem. Phys. Lett*. **1998**, *296*, 253.
(32) Demontis, P.; Suffritti, G. B. *J. Phys. Chem. B* **1997**, *101*, 5789.
(33) Baerlocher, C.; Meier, W. M.; Olson, D. H. *Atlas of Zeolite Framework Types*, 5th ed.; Elsevier: Amsterdam, 2000.
(34) Fritzsche, S. Untersuchung ausgewählter Nichtgleichgewichtsvorgänge in Vielteilchensystemen mittels statistischer Physik und Computersimulationen. Habilitation Thesis, University of Leipzig, Leipzig, Germany, 1998.
(35) Fritzsche, S.; Haberlandt, R.; Kärger, J.; Pfeifer, H.; Heinzinger, K. *Chem. Phys. Lett.* **1992**, *198*, 283.
(36) Coppens, O. M.; Bell, A. T.; Chakraborty, A. K. *Chem. Eng. Sci*. **1998**, *53*, 2053.
(37) Kar, S.; Chakravarty, C. *J. Phys. Chem. A* **2001**, *105*, 5785.
(38) Skoulidas, A. I.; Sholl, D. S. *J. Phys. Chem. B* **2002**, *106*, 5058.